



1 **Air pollution measurement errors: Is your data fit for** 2 **purpose?**

3 Sebastian Diez¹, Stuart Lacy¹, Thomas J. Bannan², Michael Flynn², Tom Gardiner³, David
4 Harrison⁴, Nicholas Marsden², Nick Martin³, Katie Read^{1,5}, Pete M. Edwards¹

5 ¹Wolfson Atmospheric Chemistry Laboratories, University of York, York, YO10 5DD, UK

6 ²Department of Earth and Environmental Science, Centre for Atmospheric Science, School of Natural Sciences,
7 The University of Manchester, Manchester, M13 9PL, UK

8 ³National Physical Laboratory, Teddington TW11 0LW, UK

9 ⁴Bureau Veritas UK, London, E1 8HG, UK

10 ⁵National Centre for Atmospheric Science, University of York, York, YO10 5DD, UK

11 *Correspondence:*

12 Sebastian Diez (sebastian.diez@york.ac.uk); Pete Edwards (pete.edwards@york.ac.uk)

13 **Abstract.** When making measurements of air quality, having a reliable estimate of the measurement uncertainty
14 is key to assessing the information content that an instrument is capable of providing, and thus its usefulness in a
15 particular application. This is especially important given the widespread emergence of Low Cost Sensors (LCS)
16 to measure air quality. To do this, end users need to clearly identify the data requirements a priori and design
17 quantifiable success criteria by which to judge the data. All measurements suffer from errors, with the degree to
18 which these impact the accuracy of the final data often determined by our ability to identify and correct for them.
19 The advent of LCS has provided a challenge in that many error sources show high spatial and temporal variability,
20 making laboratory derived corrections difficult. Characterizing LCS performance thus currently depends primarily
21 on colocation studies with reference instruments, which are very expensive and do not offer a definitive solution
22 but rather a glimpse of LCS performance in specific conditions over a limited period of time. Despite the
23 limitations, colocation studies do provide useful information on measurement device error structure, but the results
24 are non-trivial to interpret and often difficult to extrapolate to future device performance. A problem that obscures
25 much of the information content of these colocation performance assessments is the exacerbated use of global
26 performance metrics (R^2 , RMSE, MAE, etc.). Colocation studies are complex and time-consuming, and it is easy
27 to fall into the temptation to only use these metrics when trying to define the most appropriate sensor technology
28 to subsequently use. But the use of these metrics can be limited, and even misleading, restricting our understanding
29 of the error structure and therefore the measurements' information content. In this work, the nature of common
30 air pollution measurement errors is investigated, and the implications these have on traditional metrics and other
31 empirical, potentially more insightful, approaches to assess measurement performance. With this insight we
32 demonstrate the impact these errors can have on measurements, using a selection of LCS deployed alongside
33 reference measurements as part of the QUANT project, and discuss the implications this has on device end-use.



34 **Keywords:** air quality measurements, errors, uncertainty, information content, low-cost sensors.

35 1. Introduction

36 The measurement of air pollutants is central to our ability to both devise and assess the effectiveness of policies
37 to improve air quality and reduce human exposure (Molina & Molina, 2004). The emergence of low-cost sensor
38 (LCS) based technologies means a growing number of measurement devices are now available for this purpose
39 (Morawska et al., 2018), ranging from small low-cost devices that can be carried on an individual's person all the
40 way through to large, expensive reference and research-grade instrumentation. A key question that needs to be
41 asked when choosing a particular measurement technology is whether the data provided is fit for purpose
42 (Andrewes et al., 2021; Lewis & Edwards, 2016). In order to answer this, the user must first clearly define the
43 question that is to be asked of the data, and thus the information required. For example, a measurement to
44 characterize “rush hour” concentrations, or to determine if the concentration of a pollutant exceeded an 8 h average
45 legal threshold value at a particular location would demand a very different set of data requirements than a
46 measurement to determine if a change in policy had modified the average pollutant concentration trend in a
47 neighbourhood. Considerations such as measurement time resolution and ability to capture spatial variability
48 would be important for such examples (Feinberg et al., 2019). The measurement uncertainty is also of critical
49 consideration, as this ultimately determines the information content of the data, and hence how it can be used
50 (Tian et al., 2016).

51 All measurements have an associated uncertainty, and even in highly controlled laboratory assessments, the true
52 value is not known, with any measurement error defined relative to our best estimate of the range of possible true
53 values. However, quantifying and representing error and uncertainty is a challenge for a wide range of analytical
54 fields, and often what these concepts represent is not the same to all practitioners. This results in a spectrum of
55 definitions that take into account the way truth, error, and uncertainty are conceived (Cross et al., 2017; Grégis,
56 2019; Kirkham et al., 2018; Mari et al., 2021). For atmospheric measurements assessing uncertainty is complex
57 and non-trivial. Firstly, given the “true” value can never be known, an agreed reference is needed. Secondly, the
58 constantly changing atmospheric composition means that repeat measurements cannot be made and the traditional
59 methods for determining the random uncertainty are not applicable. And finally, a major challenge arises from the
60 multiple sources of error both internal and external to the sensor that can affect a measurement. Signal responses
61 from a non-target chemical or physical parameter or electromagnetic interference are examples of an almost
62 limitless number of potential sources of measurement error. In this work, we will follow the definitions given by
63 the International Vocabulary of Metrology (JCGM, 2012) for measurement error (“measured quantity value minus
64 a reference quantity value”) and for measurement uncertainty (“non-negative parameter characterizing the
65 dispersion of the quantity values being attributed to a measurand, based on the information used”).

66 The difficulties in defining and quantifying uncertainty across the full range of end-use applications of a
67 measurement device, means that often the quoted measurement uncertainty is not applicable, or in some cases not
68 provided or provided in an ambiguous manner. This makes assessing the applicability of a measurement device
69 to a particular task difficult for end-users. In this work, we investigate the nature of common air pollution
70 measurement errors, and the implications these have on traditional goodness-of-fit metrics and other, potentially
71 more insightful approaches to assess measurement uncertainty. We then use this insight to demonstrate the impact



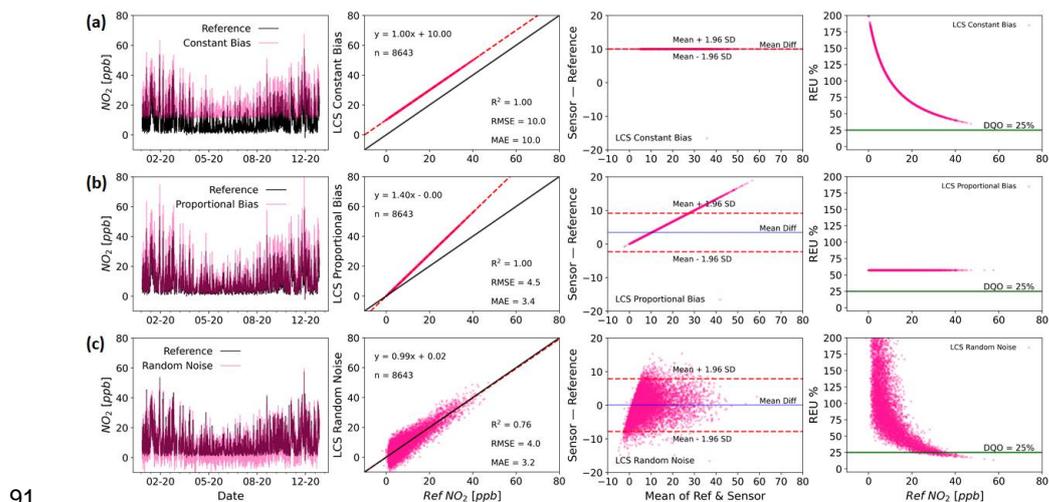
72 these errors can have on measurements, using a selection of LCS deployed alongside reference measurements as
 73 part of the UK Clean Air program funded QUANT (Quantification of Utility of Atmospheric Network
 74 Technologies) project, a 2 year collocation study of 26 commercial LCS devices (56 gases measurements and 56
 75 PM measurements) at multiple urban, background and roadside, locations in the UK. After analysing some of the
 76 real-life uncertainty characteristics we discuss the implications this has on data use.

77 2. Error characterization

78 When characterizing measurement error, in the absence of evidence to the contrary it is often assumed a linear
 79 additive model. Once the analytical form of the model is defined, its parameters aim to capture the error
 80 characteristics, and in the case of linear models (Eq. (1)), these are typically separated into three types (Tian et al.,
 81 2016): (i) proportional bias or scale error (b_1), (ii) constant bias or displacement error (b_0) and (iii) random error
 82 (ε) (Tian et al., 2016). Any measurement (y_i , e.g from the LCS) can therefore be thought of as a combination of
 83 the reference value (x_i) and the three error types, such that:

$$84 \quad y_i = b_1 x_i + b_0 + \varepsilon \quad (1)$$

85 As the simplest approximation, this linear relationship for the error characteristics is often used to correct for
 86 observed deviations between measurements and the agreed reference. It is worth to note, however, that this
 87 equation assumes time-independent error contributions and that the three error components are not correlated,
 88 which is often not the case on both counts (e.g. responses to non-target compounds). The parameter values
 89 determined for Eq. (1) are also generally only applicable for individual instruments, potentially in specific
 90 environments, unless the transferability of these parameters between devices has been explicitly demonstrated.



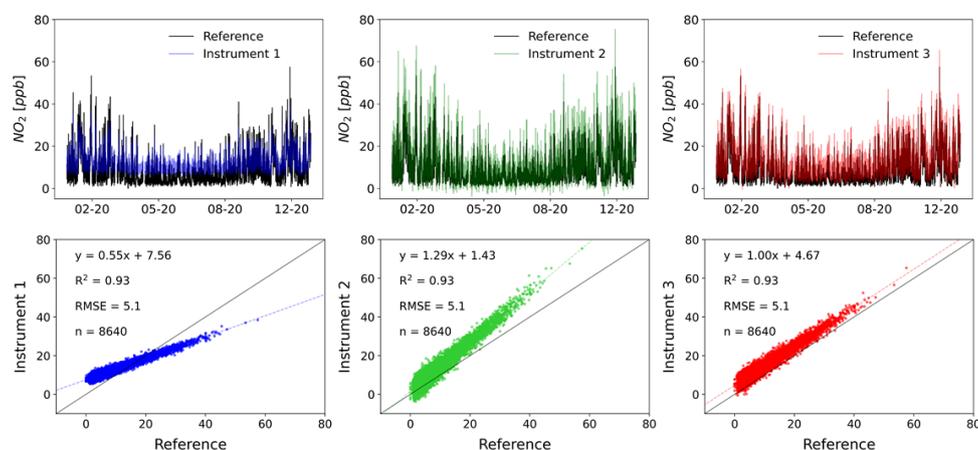
91
 92 **Figure 1.** Time series (left panels), regression plots (middle-left panels), Bland-Altman plots (middle-right panels) and
 93 **REU** (right panels, **DQO** for **NO₂** = 25%) for arbitrary examples of pure constant bias (Slope = 1, Intercept = 1, SD_ε =
 94 **0**; a-panels), pure proportional bias (Slope = 1.4, Intercept = 0, SD_ε = 0; b-panels) and pure random noise (Slope = 1,
 95 **Intercept = 0, SD_ε = 4**; c-panels) simulated errors.



96 Figure 1 shows examples of how pure constant bias (a-panels), pure proportional bias (b-panels), and pure random
97 noise (c-panels) would look like. In each of these ideal cases, the error plots enable the practitioner to view the
98 error characteristics in slightly different ways, allowing the impacts of the observed measurement uncertainty to
99 be placed into the context of the data requirements. In this work, we will refer to them as “error types” (in contrast
100 to “error sources”), which is the way they are distilled by the linear error model.

101 2.1 Performance indices, error structure and uncertainty

102 A major challenge faced by end-users of measurement devices characterised using collocation studies is the non-
103 trivial question of how the comparisons themselves are performed and how the data is communicated. Often single
104 value performance metrics, such as the coefficient of determination (R^2) or root mean squared error (RMSE), are
105 calculated between the assessed method (e.g. LCS) and an agreed reference, and the user is expected to infer an
106 expected device performance or uncertainty for a measurement in their application (Cross et al., 2017; Duvall et
107 al., 2016; Malings et al., 2019). These metrics contain useful information about the measurement, but they are
108 unable to fully describe the error characteristics, in part because they reduce the error down to a single value (Tian
109 et al., 2016). Unfortunately, the widespread use of a small number of metrics as the sole method to assess
110 measurement uncertainty, without a thorough consideration of the nature of the measurement errors, means
111 measurement devices are often chosen that are unable to provide data that is fit for purpose. In addition,
112 unconscious about potential flaws, users (e.g. researchers) could communicate findings or guide decision making
113 based on results that may not justify the conclusions drawn from the data. Figure 2 shows three simulated
114 measurements compared with the true values. Despite the measurements having identical R^2 and RMSE values,
115 the time series and regression plots show that the error characteristics are significantly different, and would impact
116 how the data from such a device could viably be used.



117
118 **Figure 2.** Time series (upper panels) and regression plots (lower panels) for three hypothetical instruments and a
119 reference. The most used metrics for evaluating the performance of LCS (R^2 and RMSE) are identical for the systems
120 shown, even when the errors have very different characteristics (time res 1 h).

121 There are multiple performance metrics that can be used for the assessment of measurement errors and uncertainty.
122 Tian et al (2016) present an excellent summary of some of the major pitfalls of performance metrics and promote



123 an approach of error modelling as a more reliable method of uncertainty quantification. These modelling
124 approaches, however, rely on the assumption of statistical stationarity, whereby the statistical properties of the
125 error are constant in the temporal and spatial domains. The presence of unknown or poorly characterised sources
126 of error, for example, due to interferences from other atmospheric constituents or drifts in sensor behaviour, makes
127 this assumption difficult to satisfy, especially when the dependencies of these errors show high spatial and
128 temporal variability. Thus, if field collocation studies are the primary method for performance assessment, as is
129 the case for LCS, only through a detailed assessment of the measurement errors across a wide range of conditions
130 and timescales can the uncertainty of the measurement be realistically estimated.

131 **2.2 Dealing with errors: established techniques vs Low-Cost Sensors**

132 Different approaches are available to the user to minimise the impact of errors, generally by making corrections
133 to the sensor data. For example, in the case of many atmospheric gas analysers, if the error is dominated by a
134 proportional bias, a multi-point calibration can be performed using standard additions of the target gas.
135 Displacement errors can be quantified, and then corrected for, by sampling a gas stream that contains zero target
136 gas. And random errors can be reduced by applying a smoothing filter (e.g moving average filter, time-averaging
137 the data, etc.), at the cost of losing some information (Brown et al., 2008). These approaches work well for simple
138 error sources that, ideally, do not change significantly over timescales from days to months. Unfortunately, more
139 complex error sources can manifest in such a way that they contribute across all three error types, and also vary
140 temporally and spatially. For example, an interference from another gas-phase compound could in part manifest
141 itself as a displacement error, based on the instrument response to its background value, and in part as a
142 proportional bias if its concentration correlates with the target compounds, with any short-term deviations from
143 perfect correlation contributing to the random error component. In this case, time-averaging combined with
144 periodic calibrations and zeros would not necessarily minimise the error, and the user would need to employ
145 different tactics. One option would be to independently measure the interferent concentration, albeit with
146 associated uncertainty, and then use this to derive a correction. This is feasible if a simple and cost-effective
147 method exists for quantifying the interferent and its influence on the result is understood, but can make it very
148 difficult to separate out error sources, and can become increasingly complex if this measurement also suffers from
149 other interferences.

150 For many measurement devices, in particular for LCS based instruments, a major challenge is that the sources and
151 nature of all the errors are unknown or difficult to quantify across all possible end-use applications, meaning
152 estimates of measurement uncertainty are difficult. In the case of most established research and reference-grade
153 measurement techniques, comprehensive laboratory and field experiments have been used to explore the nature
154 of the measurement errors (Gerboles et al., 2003; Zucco et al., 2003). Calibrations have then been developed,
155 where traceable standards are sampled and measurement bias, both constant and proportional, can be corrected
156 for. Interferences from variables such as temperature, humidity, or other gases, have also been identified and then
157 either a solution engineered to minimise their effect or robust data corrections derived. Unfortunately, these
158 approaches have been shown not to perform well in the assessment of LCS measurement errors, due to the
159 presence of multiple, potentially unknown, sensor interferences from other atmospheric constituents (Thompson
160 & Ellison, 2005). These significant sensitivities to constituents such as water vapour and other gases mean
161 laboratory-based calibrations of LCS become exceedingly complex, and expensive, as they attempt to simulate



162 the true atmospheric complexity, often resulting in observed errors being very different to real-world sampling
163 (Rai et al., 2017; Williams, 2020). This has resulted in colocation calibration becoming the accepted method for
164 characterizing LCS measurement uncertainties (De Vito et al., 2020; Masson et al., 2015; Mead et al., 2013;
165 Popoola et al., 2016; Sun et al., 2017), where sensor devices are run alongside traditional reference measurement
166 systems for a period of time, and statistical corrections derived to minimise the error between the two. As the true
167 value of a pollutant concentration cannot be known, this colocation approach assumes all the error is in the low-
168 cost measurement. Although this assumption may often be approximately valid (i.e. reference error variance \ll
169 LCS error variance), no measurement is absent of uncertainty and this can be transferred from one measurement
170 to another, obscuring attempts to identify its sources and characteristics. A further consideration when the fast
171 time-response aspect of LCS data is important, is that reference measurement uncertainties are generally
172 characterised at significantly lower reported measurement frequencies (typically 1 hr). This means that a high
173 time-resolution (e.g. 1 min) reference uncertainty must be characterized in order to accurately estimate the LCS
174 uncertainty (requiring specific experiments and additional costs). If a lower time-resolution reference data is used
175 as a proxy, then the natural variability timescales of the target compound should be known and any impact of this
176 on the reported uncertainty caveated.

177 Another challenge with this approach is that, unlike targeted laboratory studies, real-world colocation studies at a
178 single location, and for a limited time period, are not able to expose the measurement devices to the full range of
179 potential sampling conditions. As many error sources are variable, both spatially and temporally, using data
180 generated under a limited set of conditions to predict the uncertainty on future measurements is risky. Deploying
181 a statistical model makes the tacit assumption that all factors affecting the target variable are captured by the
182 model (and the data set used to build the model). This is very often an unrealistic demand, and in the complex
183 multifaceted system that is atmospheric chemistry, this is extremely unlikely to be tenable, resulting in a clear
184 potential for overfitting to the training dataset. Ultimately, however, these colocation comparisons with
185 instruments with a well-quantified uncertainty need to be able to communicate a usable estimate of the information
186 content of the data to end-users, so that devices can be chosen that are fit for a particular measurement purpose.

187 3. Methods

188 In this work, we explore measurement errors, and their impacts, using the most common single value metrics (R^2 ,
189 RMSE and MAE), along with two additional widely used approaches to visualize the error across a dataset: the
190 Bland-Altman plots (B-A) and Relative Expanded Uncertainty (REU).

191 The performance metrics provide a single value irrespective of the size of the dataset, and might appear convenient
192 for users when comparing across devices or datasets, but can encourage over-reliance on the metric, often at the
193 expense of looking at the data in more detail or bringing an awareness of the likely physical processes driving the
194 error sources. On the other hand, the B-A and the REU plots are more laborious techniques and the interpretation
195 can be challenging for non-experts, but they provide additional insights into the nature of the errors, not attainable
196 by one or more combined performance metrics.

197 In order to understand how the different tools used here show different characteristics of the error structure, some
198 errors commonly found in LCS are examined through simulation studies. Subsequently, two real world case



199 studies are presented: (i) LCS duplicates for NO₂ and PM_{2.5} belonging to the QUANT project located in two sites
200 -the Manchester Natural Environment Research Council (NERC) measurement Supersite, and the York Fishergate
201 Automatic Urban and Rural Network (AURN) roadside site- and (ii) a set of duplicate reference instruments (only
202 at Manchester Supersite). Table S1 shows the research grade instrumentation used for this study.

203 3.1 Visualization tools

204 An ideal performance metric should be able to deliver not only a performance index but also an idea of the
205 uncertainty distribution (Chai & Draxler, 2014). This is difficult to deliver through a simple numerical value, and
206 easy to interpret visualisations of the data are often much more useful for conveying multiple aspects of data
207 performance. Figure 2 shows the two most common data visualisation tools, the time-series plot and the regression
208 plot. In the time series plot the instrument under analysis and the agreed reference are plotted together as a function
209 of time. This allows a user to visually assess tendencies of over or under prediction, differences in the base line
210 or other issues, but can be readily over interpreted and does not allow for easy quantification of the observed
211 errors. In the regression plot the data from the instrument under analysis is plotted against the agreed reference
212 data. This allows for the correlation between the two methods to be more readily interpreted, in particular any
213 deviations from linearity, but gives little detail on the nature of the errors themselves.

214 In contrast to the regression plot, Bland-Altman (B-A) plots essentially display the difference between
215 measurements, enabling more information on the nature of the error to be communicated. B-A plots (Altman &
216 Bland, 1983) are extensively used in analytical chemistry and biomedicine to evaluate the differences between
217 two measurement techniques (Doğan, 2018). The B-A is a scatter plot, in which the abscissa represents the average
218 of these measures (e.g LCS and a reference measurement), acknowledging that the true value is unknown and that
219 both measurements have errors, and the ordinate shows the difference between the two paired measurements. In
220 the case where all the error is assumed to be in one of the measurements, e.g. comparing a LCS to a reference
221 grade measurement, there is an argument that the B-A abscissa could be the agreed reference value instead of the
222 average of two measurements. However, in this work we use the average of the two values as per the traditional
223 B-A analysis. To illustrate the B-A interpretation, from the error model (Eq. (1)) we can derive the following
224 expression:

$$225 \quad y_i - x_i = x_i (b_1 - 1) + b_0 + \varepsilon \quad (2)$$

226 From Eq. (2) it can be seen that if $b_1 \neq 1$ or if the error term (ε) variance is non-constant (e.g. heteroscedasticity)
227 the difference will not be normally distributed. The B-A plot (with x_i as the reference instrument results) allows a
228 quick visual assessment of the error distribution without the need to calculate the model parameters. In the case
229 the differences are normally distributed, the so-called “agreement interval” (usually defined as $\pm 2\sigma$ around the
230 mean) will hold 95% of the data points. Even though the estimated limits of agreement will be biased if the
231 differences are not normally distributed, it can still be a valuable indicator of agreement between the two
232 measurements.

233 If the ultimate goal of studying measurement errors is to diagnose the measurement uncertainty in a particular
234 target measurement range, then visualising the uncertainty in pollutant concentration space can be very
235 informative. The REU (GDE, 2010) provides a relative measure of the uncertainty interval about the measurement



236 within which the true value can be confidently asserted to lie. The abscissa in an REU plot represents the agreed
237 reference pollutant concentration, whose error is taken into account, something not considered by the other metrics
238 or visualisations discussed. The REU is regularly used to assess measurement compliance with the Data Quality
239 Objective (DQO) of the European Air Quality Directive 2008/50/EC, and is mandatory for the demonstration of
240 equivalence of methods other than the EU reference methods. For LCS the REU is widely used as a performance
241 indicator (Bagkis et al., 2021; Bigi et al., 2018; Castell et al., 2017; Cordero et al., 2018; Spinelle et al., 2015).
242 However, the evaluation of this metric is perceived as arduous and cumbersome and it is not included in the
243 majority of sensor studies (Karagulian et al., 2019). There is now a new published European Technical
244 Specification (TS) for evaluating the LCS performance for gaseous pollutants (CEN/TS 17660-1:2021). It
245 categorizes the devices in 3 classes according to the DQO (Class 1 for “indicative measurements”, Class 2 for
246 “objective estimations”, and Class 3 for non-regulatory purposes, e.g. research, education, citizen science, etc.).

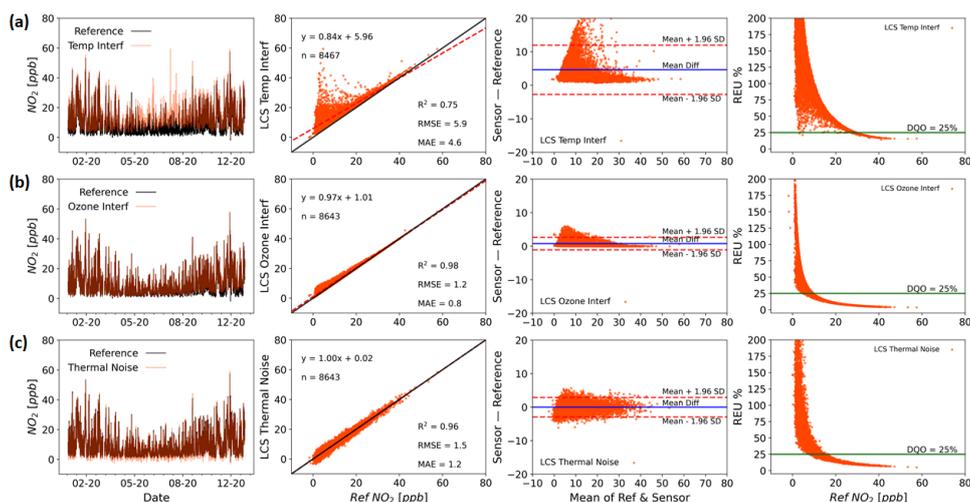
247 In the following sections, we use these established methods for assessing measurement uncertainty, alongside
248 simple time series and regression plots, to explore different error sources and their implications for air pollution
249 measurements.

250 4. Case studies

251 4.1 Simulated instruments

252 In order to investigate the impact of different origins of measurement error on measurement performance, a set of
253 simulated datasets have been created. These data are derived using real-world reference data as the true values,
254 with the subsequent addition of errors of different origins to generate the simulated measurement data. Error
255 origins were chosen for which examples have been described in the LCS literature. Performance metrics along
256 with visualization methods are then used to assess measurement performance.

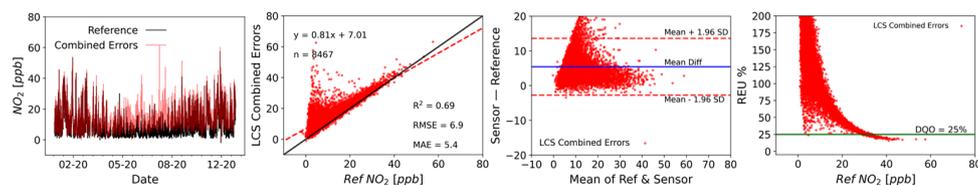
257 As the complexity of the error increases, the impact of the assumption of statistical stationarity can become more
258 difficult to satisfy, with the magnitude of the errors becoming less uniform across the observed concentration, and
259 hence spatial, or time domains. Figure 3 shows examples of modelled sources of errors on NO₂ measurements:
260 temperature interference (correction model taken from (Popoola et al., 2016), a-panels), a non-target gas (ozone)
261 interference (correction model taken from (Peters et al., 2021), b-panels) and thermal electrical noise (white noise,
262 c-panels).



263
264 **Figure 3.** Time series (left panels), regression plots (middle-left panels, including R^2 , RMSE & MAE), Bland-Altman
265 plots (middle-right panels) and REU (right panels, DQO for $\text{NO}_2 = 25\%$) for temperature (a-panels), ozone (b- panels)
266 and thermal electrical noise (c-panels) modelled interferences on NO_2 measurements (time res 1 h).

267 The above simulations show examples of how individual sources of error can impact measurement performance.
268 Figure S1 shows some more examples, this time for different drift effects (baseline drift, temperature interference
269 drift and instrument sensitivity drift). This set of error origins is not exhaustive, with countless others potentially
270 impacting the measurement, such as those coming from (i) hardware (sensor-production variability, sampling,
271 thermal effects due to materials expansion, drift due to ageing, RTC lag, Analog-to-Digital conversion,
272 electromagnetic interference, etc.), (ii) software (signal sampling frequency, signal-to-concentration conversion,
273 concept drift, etc.), (iii) sensor technology/measurement method (selectivity, sensitivity, environmental
274 interferences, etc.) and (iv) local effects (spatio-temporal variation of concentrations, turbulence, sampling issues
275 etc.).

276 Each error source impacts the uncertainty of the measurement, which in turn impacts its ability to provide useful
277 information for a particular task. For example, the form of the temperature interference shown in Fig. 3 (a-panels)
278 results in the largest errors being seen at the lower NO_2 values. This is because NO_2 concentrations are generally
279 lowest during the day, due to photolytic loss when temperatures are highest. Thus this device would be better
280 suited to an end-user intending to assess daily peak NO_2 concentration compared with the daytime hourly exposure
281 values, providing the environment the device was deployed in showed a similar relationship between temperature
282 and true NO_2 as that used here. The O_3 interference shown in Fig. 3 (b-panels) is similar, due again to a general
283 anti-correlation observed between ambient O_3 and NO_2 concentrations. This type of interference can often be
284 interpreted incorrectly as a proportional bias, and a slope correction applied to the data. However, this type of
285 correction will ultimately fail as O_3 concentrations are dependent on a range of factors, such as hydrocarbon
286 concentrations and solar radiation, and as these change the O_3 concentration relative to the NO_2 concentration will
287 change. To further complicate matters, multiple error sources can act simultaneously, meaning that the majority
288 of measurements will contain multiple sources of error. Figure 4 shows a simple linear combination of the
289 modelled errors shown in Fig 3, and the impact this has on the performance metrics.



290
291 **Figure 4. Time series (left panel), regression plot (middle-left panel, including R^2 , RMSE & MAE), Bland-Altman**
292 **plot (middle-right panel) and REU (right panel, DQO for $\text{NO}_2 = 25\%$) for a linear combination of temperature, ozone**
293 **and thermal electrical noise modelled interferences (time res 1 h).**

294 As the simulations show, the nature of the errors determine the observed effect on the measurement performance.
295 In an ideal situation, like those shown in figures 3 and 4, the error sources would be well characterised, allowing
296 the error to be modelled and approaches such as calibrations (for bias) and smoothing (for random errors)
297 employed to minimise the total uncertainty. Unfortunately, in scenarios where sources of error and their
298 characteristics are not known, modelling the error becomes more difficult and a more empirical approach to
299 assessing the measurement performance and uncertainty may be required. The growing use of LCS represents a
300 particular challenge in this regard. The susceptibility of LCS to multiple, often unknown or poorly characterised,
301 error sources means that in order to determine if a particular LCS is able to provide data with the required level
302 of uncertainty for a given task, a relevant uncertainty assessment is required. The following section explores the
303 uncertainty characteristics of several LCS, with unknown error sources, deployed alongside reference
304 instrumentation in UK urban environments as part of the QUANT study.

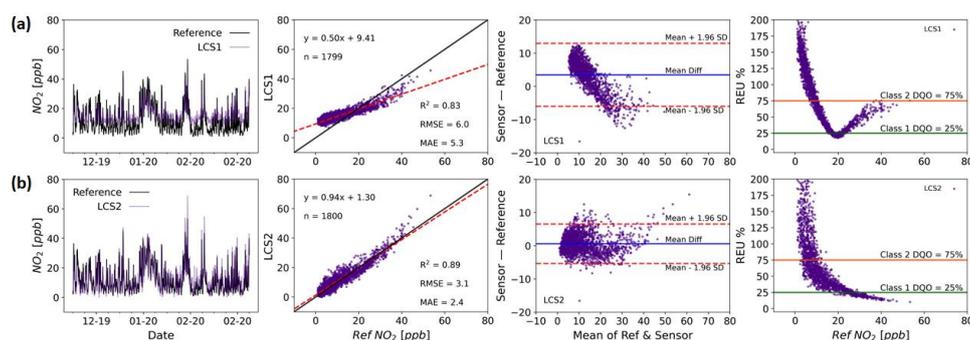
305 4.2 Real-world instruments

306 The difficulty in generating representative laboratory error characterisation data means for many measurement
307 devices the error sources are essentially unknown. This, combined with the use of imperfect algorithms that are
308 not available to the end-user (i.e. “black-box” models) to minimise errors, means that, colocation data is often the
309 best option available to end-users in order to assess the applicability of a measurement method for their desired
310 purpose. This is particularly the case for LCS air pollution measurement devices. In this section, we show
311 colocation data collected as part of the UK Clean Air program funded QUANT project, and use the tools described
312 above to investigate the impact of the observed errors on end-use.

313 Figure 5 shows two colocated NO_2 measurements, from two different LCS devices using only their out-of-box
314 calibrations (i.e. no colocation data from that site was used to improve performance), compared with colocated
315 reference measurements at an urban background site in the city of Manchester. Unlike the modelled instruments
316 in Sect. 4.1, the combination of error sources is unknown in this case and we can thus only assess the LCS
317 measurement performance through comparison with the reference measurements using metrics and visual tools.
318 There are obvious differences in the performance of both LCS instruments shown in Fig. 5. LCS1 (a-panels)
319 shows an appreciable difference in the time-series baseline, which can be interpreted from both the regression (b_1
320 <1) and the B-A plots as a proportional bias. This bias also impacts the REU plot, with a minimum in the region
321 where the regression best fit line crosses the 1:1 line ($\sim 17\text{ppb}$). It is worth noting that these plots do not directly
322 identify the source of the proportional bias, with sensor response to the target compound or another covarying
323 compound possible, but provides information on how much it impacts the data. For LCS2 (Fig. 5, b-panels) any

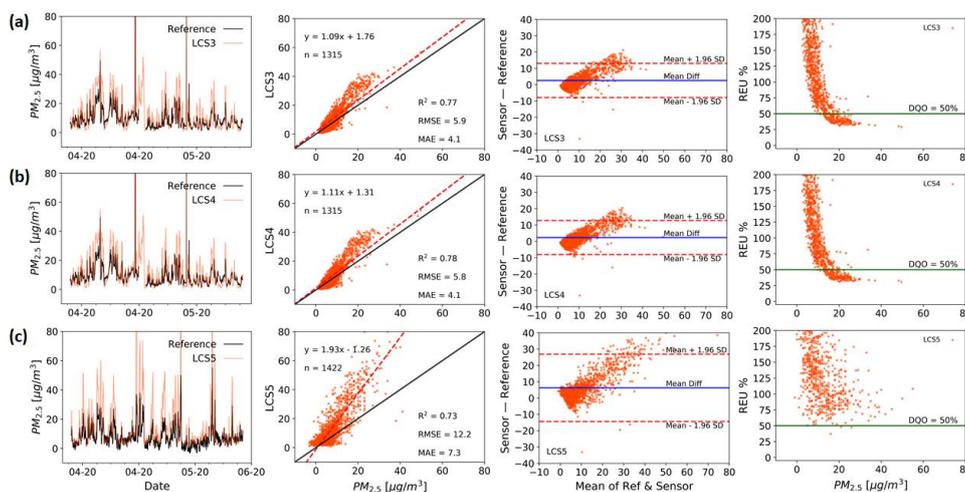


324 proportional bias is significantly smaller, with the B-A plot showing a much more symmetrical distribution of
325 points around the central line across the observed mixing ratio range, although this is not a normal distribution as
326 evidenced by the heteroscedastic nature of the differences, indicating the cause is not entirely random in nature.
327 The lack of a large proportional bias also results in the REU plot showing a continued reduction in relative
328 uncertainty as the true NO_2 concentration increases. Interestingly, both LCS's also show an additional bias at the
329 highest NO_2 values observed. This does not significantly impact the REU, due to its relative nature, but can be
330 seen in the regression and B-A plots. Correcting for the observed proportional bias in LCS1 and LCS2 improves
331 the observed performance by providing the errors with a more symmetrical distribution (LCS1* and LCS2* shown
332 in Fig. S2).



333
334 **Figure 5.** Time series (left panels), regression plots (middle-left panels), Bland-Altman plots (middle-right panels) and
335 REU (right panels; NO_2 Class 1 DQO = 25% & Class 2 DQO = 75%) for NO_2 measurements by two LCS systems of
336 different brands (a and b panels) in the same location (Manchester Supersite, December 2019 to February 2020. Time
337 res 1 h).

338 Figure 6 shows three out-of-the-box $\text{PM}_{2.5}$ measurements made by three devices from the same brand in spring,
339 located at two sites: the first two at an urban background (LCS3 & LCS4, a and b panels) and the third at a roadside
340 (LCS5, c panels). As the regression and the B-A plots show, all LCS measurements in Fig. 6 have a proportional
341 bias compared with the reference, with the LCS over predicting the reference values. Both LCS's at the urban
342 background site show very similar performance, indicating that the devices are similarly affected by errors. This
343 internal consistency is highly desirable, especially when LCS's are to be deployed in networks, as although mean
344 absolute measurement error may be high, differences between identical devices are likely to be interpretable.



345
 346 **Figure 6. Time series (left panels), regression plots (middle-left panels), Bland-Altman plots (middle-right panels) and**
 347 **REU (right panels, DQO for $PM_{2.5} = 50\%$) for $PM_{2.5}$ measurements by three LCS systems of the same brand (panels a,**
 348 **b and c) in different locations: an urban background (Manchester Supersite, panels a and b) and a roadside site (York,**
 349 **panel c) (April & May 2020, time res 1 h).**

350 The LCS data from the roadside location (LCS5) show significantly lower precision than those at the urban
 351 background site, as seen in the B-A plot. This could be caused by differences in particle properties and size
 352 distributions between the two sites (Gramsch et al., 2021), and by the high frequency variation of transport
 353 emissions close to the roadside side and turbulence effects (Baldauf et al., 2009; Makar et al., 2021). Duplicate
 354 measurements show that all sensors of this type responded similarly in this roadside environment (not shown
 355 here), supporting the high internal consistency of this device, but indicating a spatial heterogeneity in some key
 356 error sources. It is also worth noting that the gold standard instruments at the two sites are not “reference method”
 357 but “reference equivalent methods” (GDE, 2010), each using a different measurement technique: while an optical
 358 spectrometer (Palas Fidas 200) is used in Manchester, the York instrument uses a Beta attenuation method (Met
 359 One BAM 1020), which could also potentially lead to some of the observed differences. The increased apparent
 360 random variability for LCS5, combined with the proportional bias, results in significantly higher measurement
 361 uncertainty across the observed range, as can be seen by the REU plots, with LCS5 never reaching an acceptable
 362 DQO level (50% for $PM_{2.5}$). As with the NO_2 sensors (Fig. 5), if the observed proportional bias is corrected the
 363 linearly bias-corrected sensors (Fig. S3) show a much improved comparison with the reference measurement,
 364 specially LCS5*. In this case the B-A plot now shows an error characteristic more dominated by random errors,
 365 and the REU plots shows a significant reduction, with the REU at $10 \mu g m^{-3}$ reducing from ~ 75 to $\sim 50\%$.

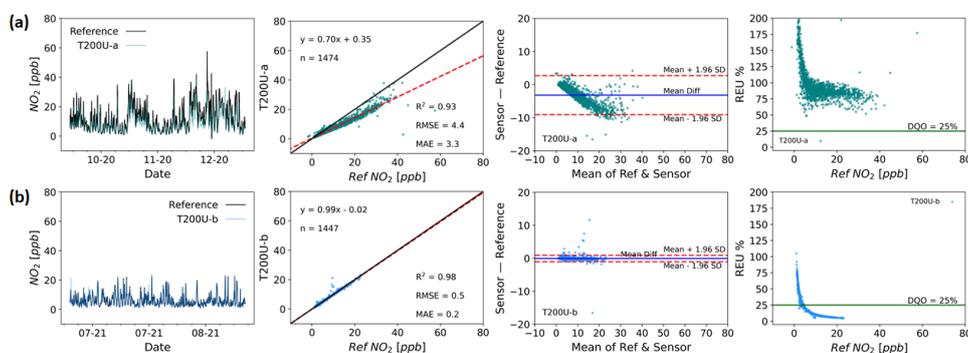
366 As a comparison for the LCS data shown above, Fig. 7 shows two identical NO_2 reference grade instruments,
 367 Teledyne T200U (Chemiluminescence method) at the Manchester urban background site (panels a and b) at during
 368 two different time periods, with a Teledyne T500U (CAPS detection method) used as the “ground truth”
 369 instrument. Instrument “a” manifests a significant proportional bias, in contrast to instrument “b”, but both show
 370 differences that could be non-negligible depending on the application. The deviations observed in instrument “a”
 371 was due to the cell pressure being above specification by $\sim 20\%$, unnoticed while the instrument was in operation.



372 This demonstrates the importance of checking instrument parameters regularly in the field even if the data appears
373 reasonable.

374 As the LCS error structure is determined relative to the performance of a reference measurement, if the reference
375 instrument suffers from significant errors this will affect the outcomes of the performance assessment, due to the
376 assumption that all the errors reside with the LCS. As Fig. 7 shows, however, this assumption is not necessarily
377 always valid and potentially argues that reference instruments used in colocation studies should be subject to
378 further error characterisation, including possible colocation with other reference instruments. As a similar
379 comparison of reference instruments, Fig. S4 shows two ozone research grade instruments (a Thermo 49i and a
380 2B).

381 It is worth noting that even when using reference, or reference equivalent, grade instrumentation, inherent
382 measurement errors mean that relative uncertainty, as shown in the REU plot, increases asymptotically at lower
383 values. This is not unexpected, but is potentially important as ambient target concentration recommendations
384 continue to fall based on updated health evidence (World Health Organization, 2021).



385
386 **Figure 7. Time series (left panel), regression plots (middle-left panel), Bland-Altman plots (middle-right panel) and**
387 **REU (right panel, DQO for NO₂ = 25%) for two identical (Teledyne T200U) reference NO₂ instruments (panels a and**
388 **b) collocated at the Manchester Supersite (1h time res). The first instrument between October & November 2020 and**
389 **the second between July & August 2021.**

390 5. Discussion

391 The widespread use of colocation studies to assess measurement device performance, means many examples exist
392 in the LCS literature where different devices are compared using summary metrics for field or laboratory studies
393 (Broday, 2017; Duvall et al., 2016; Hofman et al., 2022; Karagulian et al., 2019; Mueller et al., 2017; Rai et al.,
394 2017; van Zoest et al., 2019). Although these comparisons do provide useful information, they can be misleading
395 for end users wanting to compare the performance of different devices, as they are often carried out under different
396 conditions and do not present the data or experimental design in full. Even in the case where comparisons have
397 been done under identical conditions, the data still needs to be treated with caution, as inevitable differences
398 between assessment environment and proposed application environment, as well as any changes to
399 instrument/sensor design or data processing, mean that past performance does not guarantee future performance.



400 All measurement devices suffer from measurement errors, many of which are potentially significant depending
401 on the application, with devices and their error susceptibility covering a broad spectrum. As evidenced by Fig. 7,
402 reference instruments are not immune from this phenomena, with the proportional bias of one of the NO_x
403 instruments clearly affecting its measurements resulting in the absolute error increasing with concentration. As
404 the requirements on measurement devices continue to increase, driven in part by new evidence supporting the
405 reduction of air pollutant target values, the devices currently being used for a particular application could no longer
406 be fit-for-purpose in the situation where the limit value has decreased to the point where it is small relative to the
407 device's uncertainty.

408 Single value performance metrics, such as R^2 and RMSE, can seem convenient when comparing multiple co-
409 located devices as they facilitate decision making when a threshold criterion is defined. However, these scalar
410 values hide important information about the scale and / or distribution of the errors within a dataset; graphical
411 summaries of the measurements themselves can offer significantly more insight into the impact of measurement
412 errors on device performance and ultimate capabilities. Of particular use in air pollution measurements is the
413 ability to see how the errors manifest themselves in relation to our best estimate of the true pollutant concentration,
414 as often applications have specific target pollutant concentration ranges of interest. For example the two NO₂ LCS
415 devices shown in Fig. 5 have similar R^2 values of 0.83 and 0.89, but one is suffering from a strong proportional
416 bias that impacts on measurements either side of the 18ppb crossing-point. Errors, or combinations of errors,
417 frequently result in varying magnitude of the observed measurement inaccuracies across the concentration space
418 observed, and it is often useful to assess both the absolute and relative effects of the errors. By getting a more
419 complete picture of the device performance, decisions can be made on the effectiveness of simple corrections,
420 such as correcting for an apparent proportional bias using an assumption of a linear error model. Ultimately end
421 users need to identify the data requirements a priori and design quantifiable success criteria by which to judge the
422 data. For example, rather than just wanting to measure the 8 hour average NO₂, be more specific and require that
423 this needs to be accurate to within 5 ppb, have demonstrated approximately normally distributed errors in a
424 representative environment for the period of interest, and no statistical evidence of deviation from a linear
425 correlation with the reference measurement over the target concentration range for the period of interest.

426 A major challenge comes from complex errors, such as interferences from other compounds or with environmental
427 factors, that vary temporally and/or spatially. Similar graphical techniques to those presented above can be used
428 to identify the existence of such relationships, but correcting for them remains a challenge. This brings into
429 question the power of colocation studies, as they can ultimately never be performed under the exact conditions
430 for every intended application. The PM_{2.5} sensors shown in Fig. 6 demonstrate this, as if a colocation dataset
431 generated at the urban background site was used to inform a decision about the applicability of these devices to a
432 roadside monitoring task, then an overly optimistic assessment of the scale of the errors to be expected would be
433 likely. It is therefore always desirable that colocation studies are as relevant as possible to the desired application,
434 and this is even more paramount in the case where the error sources are poorly specified. For this reason, complete
435 meta-data on the range of conditions over which a study was conducted is key information in judging its
436 applicability to different users.

437 Although there is no strict definition on what makes a device a LCS, we often make the categorization based on
438 the hardware used. Standard reference measurement instruments are generally based on well-characterized



439 techniques developed and improved over years, based primarily on the progressive refinement of hardware (e.g.
440 materials used for the detection elements, electronic circuits to filter noise, refinement of production methods,
441 etc.). Although LCS sensor technologies are improving, it is interesting that many of the significant improvements
442 that have been made to LCS performance have been through software, rather than hardware advances. As more
443 colocation data is generated in different environments, many LCS manufacturers have been able to develop data
444 correction algorithms that minimise the scale of the errors that are present on the LCS hardware. This can greatly
445 improve the performance of LCS devices, and has been a large factor in the improvements seen in these devices
446 over recent years. These algorithms are, however, inevitably imperfect and can suffer from concept drift (De Vito
447 et al., 2020), caused by the lack of available colocation data over a full spectrum of atmospheric complexity.
448 Furthermore, any kind of statistical model introduces a new error source that can work in conjunction with the
449 pre-existing measurement errors to drastically change the observed error characteristics, making it much more
450 difficult for users to interpret and extrapolate from colocation study performance to intended application. If end
451 users are to be able to make well informed decisions about device applicability to a particular task, then an
452 argument can be made for information on the scale of the error corrections made to a reported measurement to be
453 made available, ideally alongside and a demonstration of its benefits in a relevant environment. Unfortunately,
454 this colocation data is costly to generate, meaning relevant data often does not exist, and when it does is often not
455 communicated in such a way that enables the user to make a fully informed decision.

456 6. Conclusions

457 In situ measurements of air pollutants are central to our ability to identify and mitigate poor air quality.
458 Measurement applications are wide ranging, from assessing legal compliance to quantifying the impact of an
459 intervention. The range of available measurement tools for key pollutants is also increasingly broad, with
460 instrument price tags spreading several orders of magnitude. In order for a measurement device to be of use for a
461 particular application it must be fit-for-purpose, with cost, useability and data quality all needing to be considered.
462 Understanding measurement uncertainty is key in choosing the correct tool for the job, but in order for this to be
463 assessed the job needs to be fully specified a priori. The specific data requirements of each measurement
464 application need to be understood and a measurement solution chosen that is capable of providing data with
465 sufficient information content.

466 In order to aid end users in extrapolating from colocation study performance to potential performance in a specific
467 application, performance metrics are often used. Although single value performance metrics do convey some
468 useful information about the agreement between the data from the measurement device being assessed and the
469 reference data, they can often be misleading in their evaluation of performance. This dictates a more rigorous and
470 empirical approach to data uncertainty assessment in order to determine if a measurement is fit for purpose. The
471 ability to assess device performance across the observed concentration range, as in the B-A and REU plots, enables
472 an end-user to make an informed decision about the capabilities of a measurement device in the target
473 concentration range. These visual tools also help identify any simple corrections that can be applied to improve
474 performance. In contrast, if an end-user was only provided with a single value metric, such as R^2 or RMSE then
475 it would be significantly more difficult to understand the likely implications of the measurement uncertainties.



476 All measurement devices suffer from errors, which result in deviations between the reported and true values.
477 These errors can come from a multitude of sources, with the scale of the deviation from the true value being
478 dependent on the nature of the error. Although a known measurement uncertainty for all applications would be
479 ideal for end users to be able to assess measurement device suitability for purpose, in many cases, especially for
480 LCS, this is not possible due to the presence of poorly characterised, or sometimes unknown, error sources. In the
481 absence of this, useful information on likely measurement performance can be obtained using colocation data
482 compared with a measurement with a quantified uncertainty. It is important that such a colocation study is carried
483 out in an environment as similar as possible to the application environment, as the unknown nature of many error
484 sources means their magnitude can change significantly between different locations and/or seasons (e.g. Fig. 6).
485 Ideally, depending on the measurement task, the user could use the colocation data to model the error causes and
486 use this to develop strategies to minimise final measurement uncertainty. Unfortunately, relevant colocation study
487 data is often not available, and to generate the data would be prohibitively costly, which limits the user's ability
488 to make a realistic assessment of likely uncertainties. The presence of, often complex, error minimisation post
489 processing or calibration algorithms further complicates things. This additional uncertainty is most likely to bias
490 any performance prediction if the end user is unaware of the purpose or scale of the data corrections, and their
491 applicability to the target environmental conditions. Ideally, long term colocation data sets demonstrating the
492 performance of measurement hardware and software, in a range of relevant locations, over multiple seasons, and
493 carried out by impartial bodies would be available to inform measurement solution decisions.

494 In order for end users to take full advantage of the ever increasing range of air pollution measurement devices
495 available, the questions being asked of the data must be commensurate with the information content of the data.
496 Ultimately this information content is determined by the measurement uncertainty. Thus, providing end users with
497 as accurate an estimate as possible of the likely measurement uncertainty, in any specific application, is essential
498 if end users are to be able to make informed decisions. Similarly, end users must specify the data uncertainty
499 requirements for each specific task if the correct tool for the job is to be identified. This requirement for air quality
500 management strategies to acknowledge the capabilities of available devices, both in the setting and monitoring of
501 limits, will only become increasingly important as target levels continue to decrease.

502 **Supplementary**

503 The supplement related to this article is available online.

504 **Code and data availability**

505 The QUANT intercomparison study data will be made publically available once the study has finished, in early
506 2023. In the meantime, data can be obtained upon request from the corresponding authors.

507 **Author contributions**

508 PE: Funding acquisition; Supervision. SD and PE: Project administration; Formal analysis. SD, PE & SL:
509 Conceptualization; Methodology; Investigation. SD & SL: Visualization; Software. KR, NM, MF: Resources.
510 SD, SL, KR, NM, MF: Data curation. SD, PE, SL, TB, NM, TG & DH: Writing – review & editing.

511 **Competing interests**



512 The authors declare that they have no conflict of interest.

513 Acknowledgements

514 This work was funded as part of the UKRI Strategic Priorities Fund Clean Air program (NERC NE/T00195X/1),
515 with support from Defra. We would also thank the OSCA team (Integrated Research Observation System for
516 Clean Air) at the Manchester Air Quality Supersite (MAQS), for help in data collection for the regulatory-grade
517 instruments. The secondary research grade instruments used here (Thermo ozone 49i, 2B Technologies 202 ozone,
518 and Teledyne T200U NO_x) are provided through the Atmospheric Measurement and Observation Facility
519 (AMOF) and the calibrations were carried out in the COZI Laboratory, a facility housed at the Wolfson
520 Atmospheric Chemistry Laboratories (WACL). Both funded through the National Centre for Atmospheric Science
521 (NCAS). Special thanks to Elena Martin Arenos, Chris Anthony, Killian Murphy, Stuart Young, Steve Andrews
522 and Jenny Hudson-Bell from WACL for the help and support to the project. Also thanks to Stuart Murray and
523 Chris Rhodes from the Department of Chemistry Workshop for their technical assistance and advice. Thanks to
524 Andrew Gillah and Michael Golightly from the York Council who assisted with site access.

525

526 References

- 527 Altman, D. G., & Bland, J. M. (1983). Measurement in Medicine: The Analysis of Method Comparison Studies.
528 *Journal of the Royal Statistical Society. Series D (The Statistician)*, 32(3), 307–317.
529 <https://doi.org/10.2307/2987937>
- 530 Andrewes, P., Bullock, S., Turnbull, R., & Coolbear, T. (2021). Chemical instrumental analysis versus human
531 evaluation to measure sensory properties of dairy products: What is fit for purpose? *International Dairy*
532 *Journal*, 121, 105098. <https://doi.org/10.1016/j.idairyj.2021.105098>
- 533 Bagkis, E., Kassandra, T., Karteris, M., Karteris, A., & Karatzas, K. (2021). Analyzing and Improving the
534 Performance of a Particulate Matter Low Cost Air Quality Monitoring Device. *Atmosphere*, 12(2), 251.
535 <https://doi.org/10.3390/atmos12020251>
- 536 Baldauf, R., Watkins, N., Heist, D., Bailey, C., Rowley, P., & Shores, R. (2009). Near-road air quality
537 monitoring: Factors affecting network design and interpretation of data. *Air Quality, Atmosphere &*
538 *Health*, 2(1), 1–9. <https://doi.org/10.1007/s11869-009-0028-0>
- 539 Bigi, A., Mueller, M., Grange, S. K., Ghermandi, G., & Hueglin, C. (2018). Performance of NO,
540 NO₂ and low cost sensors and three calibration approaches within a real world
541 application. *Atmospheric Measurement Techniques*, 11(6), 3717–3735. [https://doi.org/10.5194/amt-11-](https://doi.org/10.5194/amt-11-3717-2018)
542 [3717-2018](https://doi.org/10.5194/amt-11-3717-2018)



- 543 Broday, D. M. (2017). Wireless Distributed Environmental Sensor Networks for Air Pollution Measurement—
544 The Promise and the Current Reality. *Sensors (Basel, Switzerland)*, 17(10), 2263.
545 <https://doi.org/10.3390/s17102263>
- 546 Brown, R. J. C., Hood, D., & Brown, A. S. (2008). On the Optimum Sampling Time for the Measurement of
547 Pollutants in Ambient Air. *Journal of Automated Methods and Management in Chemistry*, 2008,
548 814715. <https://doi.org/10.1155/2008/814715>
- 549 Castell, N., Dauge, F. R., Schneider, P., Vogt, M., Lerner, U., Fishbain, B., Broday, D., & Bartonova, A. (2017).
550 Can commercial low-cost sensor platforms contribute to air quality monitoring and exposure estimates?
551 *Environment International*, 99, 293–302. <https://doi.org/10.1016/j.envint.2016.12.007>
- 552 CEN/TS 17660-1: 2021, Air quality – Performance evaluation of air quality sensor systems – Part 1 Gaseous
553 pollutants in ambient air.
- 554 Chai, T., & Draxler, R. R. (2014). Root mean square error (RMSE) or mean absolute error (MAE)? –
555 Arguments against avoiding RMSE in the literature. *Geoscientific Model Development*, 7(3), 1247–
556 1250. <https://doi.org/10.5194/gmd-7-1247-2014>
- 557 Cordero, J. M., Borge, R., & Narros, A. (2018). Using statistical methods to carry out in field calibrations of low
558 cost air quality sensors. *Sensors and Actuators B: Chemical*, 267, 245–254.
559 <https://doi.org/10.1016/j.snb.2018.04.021>
- 560 Cross, E. S., Williams, L. R., Lewis, D. K., Magoon, G. R., Onasch, T. B., Kaminsky, M. L., Worsnop, D. R., &
561 Jayne, J. T. (2017). Use of electrochemical sensors for measurement of air pollution: Correcting
562 interference response and validating measurements. *Atmospheric Measurement Techniques*, 10(9),
563 3575–3588. <https://doi.org/10.5194/amt-10-3575-2017>
- 564 De Vito, S., Esposito, E., Castell, N., Schneider, P., & Bartonova, A. (2020). On the robustness of field
565 calibration for smart air quality monitors. *Sensors and Actuators B: Chemical*, 310, 127869.
566 <https://doi.org/10.1016/j.snb.2020.127869>
- 567 Doğan, N. Ö. (2018). Bland-Altman analysis: A paradigm to understand correlation and agreement. *Turkish*
568 *Journal of Emergency Medicine*, 18(4), 139–141. <https://doi.org/10.1016/j.tjem.2018.09.001>
- 569 Duvall, R. M., Long, R. W., Beaver, M. R., Kronmiller, K. G., Wheeler, M. L., & Szykman, J. J. (2016).
570 Performance Evaluation and Community Application of Low-Cost Sensors for Ozone and Nitrogen
571 Dioxide. *Sensors*, 16(10), 1698. <https://doi.org/10.3390/s16101698>
- 572 Feinberg, S. N., Williams, R., Hagler, G., Low, J., Smith, L., Brown, R., Garver, D., Davis, M., Morton, M.,



- 573 Schaefer, J., & Campbell, J. (2019). Examining spatiotemporal variability of urban particulate matter
574 and application of high-time resolution data from a network of low-cost air pollution sensors.
575 *Atmospheric Environment*, 213, 579–584. <https://doi.org/10.1016/j.atmosenv.2019.06.026>
- 576 GDE. (2010). Guidance for the Demonstration of Equivalence of Ambient Air Monitoring Methods. Report by
577 an EC Working Group.
- 578 Gerboles, M., Lagler, F., Rembges, D., & Brun, C. (2003). Assessment of uncertainty of NO₂ measurements by
579 the chemiluminescence method and discussion of the quality objective of the NO₂ European Directive.
580 *Journal of Environmental Monitoring*, 5(4), 529–540. <https://doi.org/10.1039/B302358C>
- 581 Gramsch, E., Oyola, P., Reyes, F., Vásquez, Y., Rubio, M. A., Soto, C., Pérez, P., Moreno, F., & Gutiérrez, N.
582 (2021). Influence of Particle Composition and Size on the Accuracy of Low Cost PM Sensors:
583 Findings From Field Campaigns. *Frontiers in Environmental Science*, 9.
584 <https://www.frontiersin.org/article/10.3389/fenvs.2021.751267>
- 585 Grégis, F. (2019). On the meaning of measurement uncertainty. *Measurement*, 133, 41–46.
586 <https://doi.org/10.1016/j.measurement.2018.09.073>
- 587 Hofman, J., Nikolaou, M., Shantharam, S. P., Stroobants, C., Weijs, S., & La Manna, V. P. (2022). Distant
588 calibration of low-cost PM and NO₂ sensors; evidence from multiple sensor testbeds. *Atmospheric
589 Pollution Research*, 13(1), 101246. <https://doi.org/10.1016/j.apr.2021.101246>
- 590 JCGM. (2012). International vocabulary of metrology - Basic and general concepts and associated terms, Paris:
591 BIPM.
- 592 Karagulian, F., Barbieri, M., Kotsev, A., Spinelle, L., Gerboles, M., Lagler, F., Redon, N., Crunaire, S., &
593 Borowiak, A. (2019). Review of the Performance of Low-Cost Sensors for Air Quality Monitoring.
594 *Atmosphere*, 10(9), 506. <https://doi.org/10.3390/atmos10090506>
- 595 Kirkham, H., Riepnicks, A., Albu, M., & Laverty, D. (2018). The nature of measurement, and the true value of a
596 measured quantity. *2018 IEEE International Instrumentation and Measurement Technology
597 Conference (I2MTC)*, 1–6. <https://doi.org/10.1109/I2MTC.2018.8409771>
- 598 Lewis, A., & Edwards, P. (2016). Validate personal air-pollution sensors. *Nature News*, 535(7610), 29.
599 <https://doi.org/10.1038/535029a>
- 600 Makar, P. A., Stroud, C., Akingunola, A., Zhang, J., Ren, S., Cheung, P., & Zheng, Q. (2021). Vehicle-induced
601 turbulence and atmospheric pollution. *Atmospheric Chemistry and Physics*, 21(16), 12291–12316.
602 <https://doi.org/10.5194/acp-21-12291-2021>



- 603 Malings, C., Tanzer, R., Hauryliuk, A., Kumar, S. P. N., Zimmerman, N., Kara, L. B., Presto, A. A., & R.
604 Subramanian. (2019). Development of a general calibration model and long-term performance
605 evaluation of low-cost sensors for air pollutant gas monitoring. *Atmospheric Measurement Techniques*,
606 *12*(2), 903–920. <https://doi.org/10.5194/amt-12-903-2019>
- 607 Mari, L., Wilson, M., & Maul, A. (2021). *Measurement across the Sciences: Developing a Shared Concept*
608 *System for Measurement*. Springer International Publishing. <https://doi.org/10.1007/978-3-030-65558-7>
- 609 Masson, N., Piedrahita, R., & Hannigan, M. (2015). Approach for quantification of metal oxide type
610 semiconductor gas sensors used for ambient air quality monitoring. *Sensors and Actuators B:*
611 *Chemical*, *208*, 339–345. <https://doi.org/10.1016/j.snb.2014.11.032>
- 612 Matejka, J., & Fitzmaurice, G. (2017). Same Stats, Different Graphs: Generating Datasets with Varied
613 Appearance and Identical Statistics through Simulated Annealing. *Proceedings of the 2017 CHI*
614 *Conference on Human Factors in Computing Systems*, 1290–1294.
615 <https://doi.org/10.1145/3025453.3025912>
- 616 Mead, M. I., Popoola, O. A. M., Stewart, G. B., Landshoff, P., Calleja, M., Hayes, M., Baldovi, J. J., McLeod,
617 M. W., Hodgson, T. F., Dicks, J., Lewis, A., Cohen, J., Baron, R., Saffell, J. R., & Jones, R. L. (2013).
618 The use of electrochemical sensors for monitoring urban air quality in low-cost, high-density networks.
619 *Atmospheric Environment*, *70*, 186–203. <https://doi.org/10.1016/j.atmosenv.2012.11.060>
- 620 Molina, M. J., & Molina, L. T. (2004). Megacities and Atmospheric Pollution. *Journal of the Air & Waste*
621 *Management Association*, *54*(6), 644–680. <https://doi.org/10.1080/10473289.2004.10470936>
- 622 Morawska, L., Thai, P., Liu, X., Asumadu-Sakyi, A., Ayoko, G., Bartonova, A., Bedini, A., Chai, F.,
623 Christensen, B., Dunbabin, M., Gao, J., Hagler, G., Jayaratne, R., Kumar, P., Lau, A., Louie, P.,
624 Mazaheri, M., Ning, Z., Motta, N., ... Williams, R. (2018). Applications of low-cost sensing
625 technologies for air quality monitoring and exposure assessment: How far have they gone?
626 *Environment International*, *116*, 286–299. <https://doi.org/10.1016/j.envint.2018.04.018>
- 627 Mueller, M., Meyer, J., & Hueglin, C. (2017). Design of an ozone and nitrogen dioxide sensor unit and its long-
628 term operation within a sensor network in the city of Zurich. *Atmospheric Measurement Techniques*,
629 *10*(10), 3783–3799. <https://doi.org/10.5194/amt-10-3783-2017>
- 630 Peters, D. R., Popoola, O. A. M., Jones, R. L., Martin, N. A., Mills, J., Fonseca, E. R., Stidworthy, A., Forsyth,
631 E., Carruthers, D., Dupuy-Todd, M., Douglas, F., Moore, K., Shah, R. U., Padilla, L. E., & Alvarez, R.
632 A. (2021). *Evaluating uncertainty in sensor networks for urban air pollution insights* [Preprint].



- 633 Gases/In Situ Measurement/Validation and Intercomparisons. <https://doi.org/10.5194/amt-2021-210>
- 634 Popoola, O. A. M., Stewart, G. B., Mead, M. I., & Jones, R. L. (2016). Development of a baseline-temperature
635 correction methodology for electrochemical sensors and its implications for long-term stability.
636 *Atmospheric Environment*, *147*, 330–343. <https://doi.org/10.1016/j.atmosenv.2016.10.024>
- 637 Rai, A. C., Kumar, P., Pilla, F., Skouloudis, A. N., Di Sabatino, S., Ratti, C., Yasar, A., & Rickerby, D. (2017).
638 End-user perspective of low-cost sensors for outdoor air pollution monitoring. *Science of The Total*
639 *Environment*, *607–608*, 691–705. <https://doi.org/10.1016/j.scitotenv.2017.06.266>
- 640 Spinelle, L., Gerboles, M., Villani, M. G., Aleixandre, M., & Bonavitaola, F. (2015). Field calibration of a
641 cluster of low-cost available sensors for air quality monitoring. Part A: Ozone and nitrogen dioxide.
642 *Sensors and Actuators B: Chemical*, *215*, 249–257. <https://doi.org/10.1016/j.snb.2015.03.031>
- 643 Sun, L., Westerdahl, D., & Ning, Z. (2017). Development and Evaluation of A Novel and Cost-Effective
644 Approach for Low-Cost NO₂ Sensor Drift Correction. *Sensors (Basel, Switzerland)*, *17*(8), E1916.
645 <https://doi.org/10.3390/s17081916>
- 646 Thompson, M., & Ellison, S. L. R. (2005). A review of interference effects and their correction in chemical
647 analysis with special reference to uncertainty. *Accreditation and Quality Assurance*, *10*(3), 82–97.
648 <https://doi.org/10.1007/s00769-004-0871-5>
- 649 Tian, Y., Nearing, G. S., Peters-Lidard, C. D., Harrison, K. W., & Tang, L. (2016). Performance Metrics, Error
650 Modeling, and Uncertainty Quantification. *Monthly Weather Review*, *144*(2), 607–613.
651 <https://doi.org/10.1175/MWR-D-15-0087.1>
- 652 van Zoest, V., Osei, F. B., Stein, A., & Hoek, G. (2019). Calibration of low-cost NO₂ sensors in an urban air
653 quality network. *Atmospheric Environment*, *210*, 66–75.
654 <https://doi.org/10.1016/j.atmosenv.2019.04.048>
- 655 Williams, D. E. (2020). Electrochemical sensors for environmental gas analysis. *Current Opinion in*
656 *Electrochemistry*, *22*, 145–153. <https://doi.org/10.1016/j.coelec.2020.06.006>
- 657 World Health Organization. (2021). *WHO global air quality guidelines: Particulate matter (PM_{2.5} and PM₁₀),*
658 *ozone, nitrogen dioxide, sulfur dioxide and carbon monoxide: executive summary*. World Health
659 Organization. <https://apps.who.int/iris/handle/10665/345334>
- 660 Zucco, M., Curci, S., Castrofino, G., & Sassi, M. P. (2003). A comprehensive analysis of the uncertainty of a
661 commercial ozone photometer. *Measurement Science and Technology*, *14*(9), 1683–1689.
662 <https://doi.org/10.1088/0957-0233/14/9/320>